J. Membrane Biol. 141, 149–157 (1994)

The Journal of
Membrane
Biology

Ion Transport across the Early Chick Embryo: I. Electrical Measurements, Ionic Fluxes and Regional Heterogeneity

P. Kučera[1], H. Abriel[1], U. Katz[2]

[1]Institute of Physiology, Faculty of Medicine, University of Lausanne, Bugnon 7, CH-1005 Lausanne, Switzerland
[2]Department of Biology, Technion-Israel Institute of Technology, Haifa, Israel

Received: 16 December 1993/Revised: 13 April 1994

Abstract. The chick blastoderm at the stage of late gastrula is a flat disc formed by three cell layers and exhibiting epithelial properties. Blastoderms were cultured in miniature chambers and their electrophysiological characteristics were determined under Ussing conditions.

Under open-circuit condition and identical physiological solutions on both sides, spontaneous transblastodermal potential difference (V_{oc}) of -7.5 ± 3.3 mV (ventral side positive) was measured. Under short-circuit condition (transblastodermal $\Delta V = 0$ mV), the blastoderm generated short-circuit current (I_{sc}) of 21 ± 8 $\mu A/cm^2$, which was entirely dependent on extracellular sodium, sensitive to ouabain applied ventrally and independent of extracellular chloride. The net transblastodermal Na^+ flux fully accounted for the measured I_{sc}, both under control conditions and with ouabain. The total transblastodermal resistance (R_{tot}) was 390 ± 125 Ωcm^2.

Frequently, the V_{oc}, I_{sc} and R_{tot} showed spontaneous oscillations with a period of 4–5 min. Removal of endoderm and mesoderm did not significantly affect the electrical properties, indicating that the electrogenic sodium transport is generated by the ectoderm.

The V_{oc} and I_{sc} measured in the *area pellucida* (-1.3 ± 0.8 mV, 9.3 ± 4.4 $\mu A/cm^2$) and extraembryonic *area opaca* (-7.8 ± 1.1 mV, 31.2 ± 12.7 $\mu A/cm^2$) were significantly different. Such a heterogeneous distribution of electrical properties can explain the presence in the blastoderm of extracellular electrical currents found by using a vibrating probe.

Key words: Chick embryo — Epithelial characteristics — Ussing conditions — Na^+ transport

Correspondence to: P. Kučera

Introduction

The rapid cell proliferation in the earliest phase of embryonic development leads to a complex reorganization of the newly formed cells. The first example of such a reorganization is the formation of the blastocyst. During this process, the blastomeres progressively occupy the periphery of the embryo and a central cavity, i.e., the blastocoel, is formed. This process shows species-dependent particularities but is characteristic for all vertebrates (*see, for review,* Balinsky, 1981).

The formation of blastocyst depends on a progressive and parallel development of intercellular contacts and structural polarization of the embryonic cells (Fleming et al., 1989). Functional consequences of such a differentiation are the establishment of transcellular transports of ions, water and substrates from the albumen and yolk into the blastocoel cavity and thus transformation of the primary intraembryonic extracellular fluid.

It is postulated that the most important mechanism of the accumulation of the fluid in the blastocoel is the active transport of sodium followed by osmotically driven water. The presence of active sodium transport mechanism has been shown in amphibian embryos (Morill, Kostellow & Watson, 1966; Komazaki & Takada, 1988), in avian embryos (Stern & MacKenzie, 1983; Stern, Manning & Gillespie, 1985; Kučera & Katz, 1988) and especially in mammalian embryos (e.g., in the rabbit: Cross & Brinster, 1970; Smith, 1970; Cross, 1973; Powers, Borland & Biggers, 1977; Borland, 1977; Benos, 1981; in the mouse: DiZio & Tasca, 1977; Wiley, 1984; Manejwala, Cragoe & Schultz, 1989).

The amphibian and mammalian blastula and gastrula are three-dimensional structures. In the meroblastic chick embryo, where the development takes place around a relatively huge yolk mass, these developmental stages form the so-called blastoderm where the epiblast and hypoblast and, later, ectoderm and en-

doderm are flat epithelial cell layers (Balinsky, 1981). This "bi-dimensional" arrangement makes the chick embryo especially suitable for studies of early embryonic ionic transcellular transports.

Microelectrode studies in ovo showed that the ventral side of the epiblast is positive with respect to the dorsal side, and, studies in vitro (based on flux measurements in dissected epiblasts) showed that the epiblast transports actively sodium in the dorsoventral direction (Stern & MacKenzie, 1983).

However, for quantitative analysis, Ussing conditions (identical solutions on both sides, short-circuit, Ussing & Zerahn, 1951) which are used in epithelial physiology, are required. Such an approach does not only represent a mean for quantitative and qualitative comparisons with other epithelia but will allow also to examine the transporting properties of different regions of the blastoderm, namely, the extraembryonic *area opaca* and embryonic *area pellucida*. These two areas present a very early functional differentiation with respect to their energy metabolism (Raddatz & Kučera, 1983; Kučera, Raddatz & Baroffio, 1984; Raddatz, de Ribaupierre & Kučera, 1987), mechanical behavior and sensitivity to electrical stimuli (Kučera & Burnand, 1987), as well as supracellular organization of the extracellular matrix (Kučera & Monnet-Tschudi, 1987).

Therefore, we have developed an experimental setup allowing us to study the electrical properties of the early chick blastoderm which proved to be an efficient but also a heterogeneous sodium transporting tissue. Some results have already been presented as preliminary reports (Kučera & Katz, 1988; Kučera & de Ribaupierre, 1989).

Materials and Methods

Chick Blastoderms

Early stages of the chick embryo were obtained from eggs (Warren strain) preincubated for 18 to 22 hr at 37.5°C and 90% of humidity. The blastoderms corresponded to the developmental stages 4 to 6 according to Hamburger and Hamilton (1951), i.e., to the period of gastrulation and neurulation. Figure 1*A* shows a blastoderm at the stage 5 HH: it is a cellular disc, attached at its periphery to the vitelline membrane and containing the peripheral extraembryonic *area opaca* and the central *area pellucida* where the embryo develops.

Both areas are made of three cell layers, the ectoderm, mesoderm and endoderm. The ectoderm, predominant in these early stages, forms an epithelium as judged from the characteristics of cells showing clear signs of structural polarization, e.g., tight intercellular junctions, different conformation of dorsal and ventral membranes, ventral extracellular matrix. The ectodermal cells in the *area pellucida* are mostly columnar and in constant rearrangement (Fig. 1*B*) while those in the *area opaca* are rather flat, more uniform (Fig. 1*C*), and show well-differentiated intercellular junctions.

Explantation

The explantation procedure was carried out at room temperature in a Tyrode solution adapted to the chick (Kucera & Raddatz, 1980) according to data describing the composition of chick embryo fluids (Howard, 1957; Romanoff, 1967; Simkiss, 1980). The solution contained (in mM): Na^+ 109, K^+ 2.3, Ca^{2+} 1.4, Mg^{2+} 0.8, Cl^- 107.2, HCO_3^- 6.0, $H_2PO_4^-$ 0.32, glucose 7.6. The final osmolarity was 230 mOsm and pH was adjusted with 0.1 M HCl to 7.4.

The yolk was separated from the albumen and transferred into a beaker containing the solution. The vitelline membrane was circularly cut slightly above the yolk equator, and peeled off with the blastoderm remaining attached to the membrane. The membrane was stretched and fixed between two, metallic rings and yolk particles adhering to the *area opaca* were removed by a gentle stream of solution. The preparation was transferred into the culture chamber with the blastoderm located underneath the vitelline membrane.

Mounting into the Experimental Chamber

The chamber (Kučera et al., 1984) used in the present study was made from an electrically insulating material (Kelef) and closed tightly by a glass window, with a horizontal perspex separation plate (Fig. 1*D*). The plate has an exposed aperture of 4 mm in diameter surrounded by a rim over and around which the blastoderms were centered and spread by manipulating the vitelline membrane, and then fixed by using a very thin O-ring.

This delicate manipulation was done as follows. A plastic "bell" was cut from the large end of an Eppendorf (yellow) pipette tip so that its internal diameter was slightly larger than the rim supporting the embryo. The bell was suspended on a micromanipulator and the silicone O-ring (4.7 mm in diameter, 0.3 mm thick) was stretched around its inferior border. The bell was centered under binocular observation onto the preparation and slowly lowered until a slight compression of the vitelline membrane was visible. While retiring slowly the bell upward, the O-ring was simultaneously pushed down by watchmaker forceps until it sprang down and fixed elastically the preparation into the rim. The vitelline membrane was then carefully perforated and removed.

In separate experiments, the electrical parameters of each embryonic area (i.e., *area pellucida* and *opaca*) were measured using a separation plate with an aperture of 2 mm in diameter only. The mounting was delicate, but we succeeded in 10 experiments.

In the complete preparation, the blastoderm separated the volume of the chamber into upper and lower compartments (1 ml each). The dorsal side of the blastoderm faced always the upper compartment (Fig. 1*D*). Both compartments of the chamber were alternatively perfused with the Tyrode solution using a pair of push-pull syringes connected by Teflon tubes to four stop-cocks built in the body of the chamber. The rate of perfusion (0.375 ml/min) ensured laminar flow over and under the preparation. Such a flow covered largely the metabolic and buffering requirements of the embryo (Kučera et al., 1984).

The chamber was placed onto the stage of inverted microscope housed in an air incubator and maintained at 37.5°C. The embryos were photographed every hour.

Electrical Measurements

Both compartments of the chamber were connected to two pairs of chlorinated silver electrodes through agar bridges (Teflon tubes filled with 2% agar in 1 M KCl, Fig. 1*D*). Two electrodes were used to measure the potential difference across the blastoderm and the two others to inject electrical current. An automatic voltage clamp device (constructed by Van Driessche, Louvain, Belgium) was used to maintain the blastoderm in short-circuit condition ($\Delta V = 0$ mV). Thus, the blastoderms were studied according to conditions of Ussing and Zerahn (1951) in a horizontal position. The area of the blastoderm studied was 0.125 cm^2 and consisted of the whole *area pellucida* sur-

rounded by a part of the *area opaca* (Fig. 1*A*) in an average surface ratio of 1:1. The peripheral cells were always quickly and firmly adhering to the supporting rim and no signs of cell damage were present.

The blastoderms were short-circuited throughout the experiment (except for occasional measurements of the open-circuit potential) and the short-circuit current and transblastodermal potential were continuously recorded on a paper recorder and also stored in a microcomputer. The total transblastodermal electric conductance was evaluated from current responses to externally applied square voltage pulses (0.5 to 2 mV for 10 sec every 50 sec). The electrodes were regularly checked for polarization effects.

Measurements of Sodium and Chloride Fluxes

The fluxes of Na^+ and Cl^- were measured using ^{22}Na and ^{36}Cl as tracers (Amersham International, Buckinghamshire, England). The dorsal or ventral compartments were loaded with the tracers (final specific activity of the radioactive compartment was 150–225 mCi/mol for Na^+ and 150 mCi/mol for Cl^-). The "hot" compartment remained unperfused during the experiment, while the "cold" compartment was perfused with the Tyrode solution at a flow rate of 0.2 ml/min. The preparation was short-circuited ($\Delta V = 0$ mV) and the perfusate was collected each 15 min for 1.5 to 3 hr.

The samples were first counted for ^{22}Na gamma radiation in a gamma counter (Gammamatic, Kontron, Montagny le Bretonneux, France). Thereafter, 7 ml of a liquid scintillation cocktail (Ready Value, Beckman, Fullerton, CA) were added to 2 ml of the 15 min aqueous sample and the beta emission due to both ^{36}Cl and ^{22}Na was measured in a beta liquid scintillation counter (Betamatic IV, Kontron S.A., Montagny le Bretonneux, France). The ^{36}Cl counts of each sample were calculated by subtraction of the ^{22}Na counts, determined by measuring appropriate standards in both counters, from the total beta counts. These measurements were used to calculate the unidirectional fluxes of Na^+ and Cl^- in dorsoventral direction (J_{DV}) and ventrodorsal direction (J_{VD}).

Ionic Replacements and Drugs

In one series of experiments, the sodium was replaced isosmotically in various proportions by choline or magnesium. In the other series, the chloride was replaced isosmotically by sulfate, nitrate, or gluconate. All chemicals were of analytical grade. Ouabain was from Sigma, GmbH, Deisenhofen, Germany.

Statistical Analysis

The bilateral Student's *t*-test was used (paired or unpaired test depending on conditions) and the value of $P < 0.05$ adopted as criterion of statistical significance.

Results

Electrical Properties of the Chick Blastoderm

The electrical parameters summarized in Table 1 were obtained in 42 blastoderms corresponding to the developmental stages 4 to 8 HH. Although these experiments were done over two years, the results were very comparable from one series to the other. The values presented were obtained after 30 to 50 min equilibration of the embryos with the perfused Tyrode solution at 37.5°C. After this period, the electrical properties of the blastoderms stabilized for nearly 2 hr. The development of the embryo in the chamber under the short-circuit conditions ($\Delta V = 0$ mV) continued, although with a slight retard, until the formation of neural folds and 1–2 somites (i.e., until stage 8+ HH).

Under open-circuit conditions, the dorsal side of the blastoderm was negative with respect to the ventral side. The values of transblastodermal potential (V_{oc}) and short-circuit current (I_{sc}) were increasing during the warming of the preparation reaching on the average -7.5 mV and 21 μA/cm^2, respectively. The total transblastodermal conductance (G_{tot}) was decreasing and stabilized at a value of 2.6 mS/cm^2 on the average. All these steady-state values were significantly different ($P < 0.001$) from the values recorded at the starting temperature (usually 25°C). The electrical parameters were sensitive to variations in the perfusion rate in the dorsal compartment.

Figure 2 illustrates a typical record of V_{oc} and I_{sc} after the period of equilibration. Interestingly, this record presents also spontaneous and sustained regular oscillations. These slow oscillations with a period between 2.5 and 5 min were observed in more than one half of preparations.

The Current-Voltage Relationship

Clamping the preparation between -20 to $+50$ mV in steps of 10 mV lasting 5 min each, produced steady-state variations in the I_{sc} which were strictly linear. The G_{tot} determined from *I/V* relationships (*not shown*) did not differ from the G_{tot} as determined from the voltage pulses. No fast transient on-off voltage dependent responses were observed (three experiments, *results not shown*).

Developmental Changes

At the stage 4 HH (7 blastoderms), the V_{oc} and I_{sc} were -8.9 ± 3.5 mV and 20.8 ± 5.6 μA/cm^2, respectively. At the stage 6 to 8 HH (10 blastoderms), these values were -6.1 ± 2.6 mV and 16.2 ± 8.3 μA/cm^2, respectively. The difference between the open-circuit potentials was statistically significant ($P < 0.05$).

Fluxes of Sodium and Chloride

Under control conditions, the $J_{DV}^{Na^+}$ was about three times greater than the $J_{VD}^{Na^+}$ (Table 2*A*). The net dorsoventral Na^+ flux (0.70 μEq/cm^2/hr) was equivalent to 18.9 μA/cm^2. With ouabain, the flux of Na^+ was decreased in the dorsoventral direction (Fig. 3) but unchanged in the opposite direction (Table 2*A*). The net flux (0.12

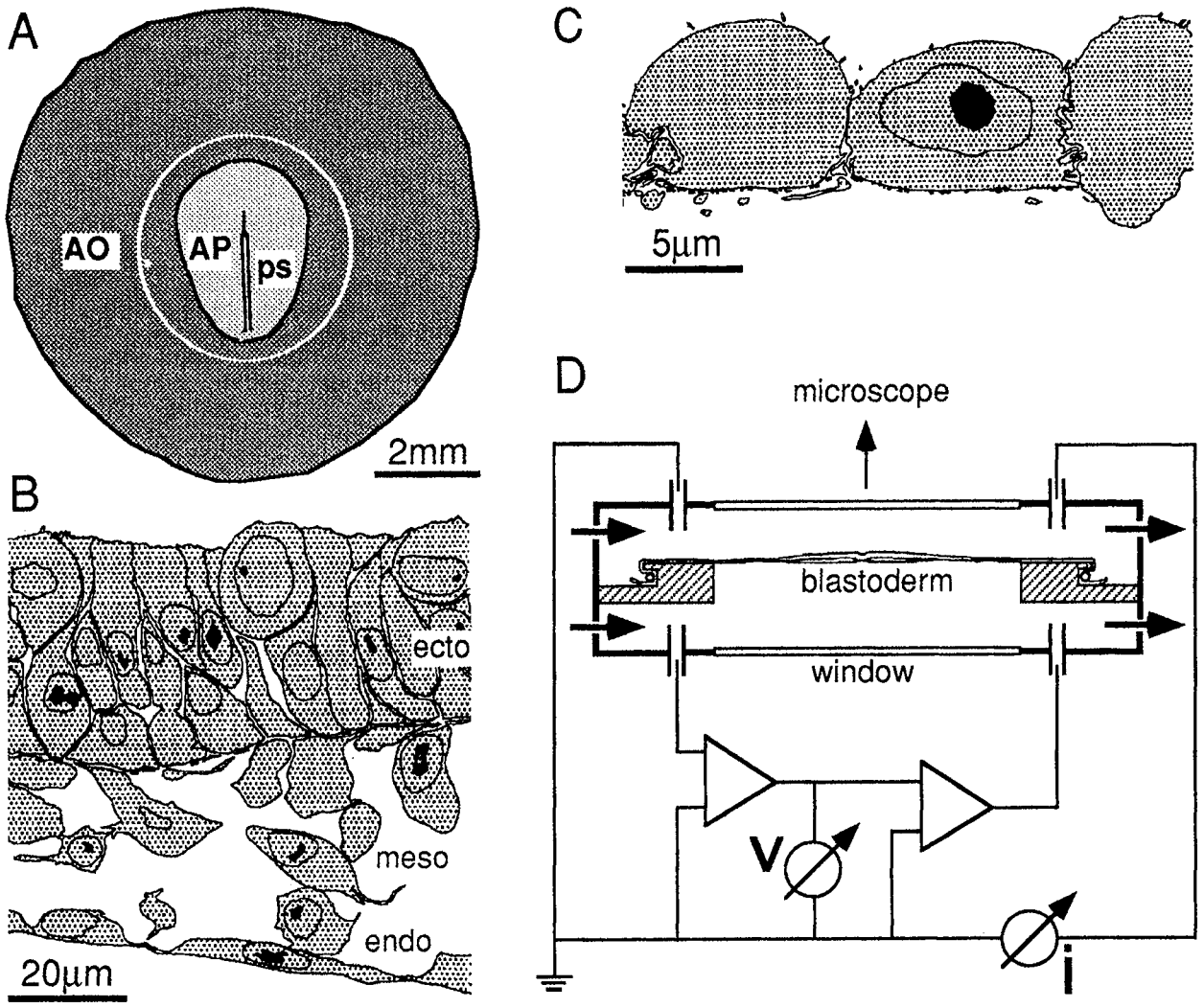

Fig. 1. The chick blastoderm and experimental set-up. (*A*) A drawing of the one-day-old chick blastoderm (stage 5 HH). (*AO*) *Area opaca,* (*AP*) *area pellucida;* (*ps*) primitive streak. The margin of AO is attached to the vitelline membrane. The white circle shows the area studied in Ussing conditions. (*B*) A section across the AP drawn after electron micrograph showing the three cell layers: ectoderm (rather loose intercellular contacts), mesoderm (individually migrating cells) and endoderm. (*C*) A section across the AO drawn after electron micrograph showing the ectodermal cells with well-developed junctional complexes. (*D*) The scheme of the embryo mounted in the Ussing-type chamber (*not to scale*). The blastoderm is fixed (dorsal side up) on the separating plate (hatched) by a fine silicone O-ring. Both compartments of the chamber are perfused (arrows) and connected through agar bridges to an automatic feedback apparatus allowing measurements of the transblastodermal potential difference (*v*) or transblastodermal current (*i*). In reality, the current electrodes are positioned symmetrically with respect to the embryo.

Table 1. Electrical properties of the early chick embryo

	n	V_{oc} (mV)	I_{sc} (µA/cm²)	G_{tot} (mS/cm²)
Control values:	21	−7.5 ± 3.3	21.2 ± 7.9	2.6 ± 0.9
Effects of			Variations in %	
Na^+-free medium	6	−100	−100	−20 ± 2
Cl^--free medium	8	ND	0	−20 ± 4
Ouabain 0.1 mM	7	−78 ± 6	−82 ± 7	−13 ± 10

V_{oc}: spontaneous open-circuit potential (V_{dorsal}-$V_{ventral}$), I_{sc}: short-circuit current, G_{tot}: total transblastodermal conductance. The values are means ± SD. *n:* number of embryos. ND: not determined.

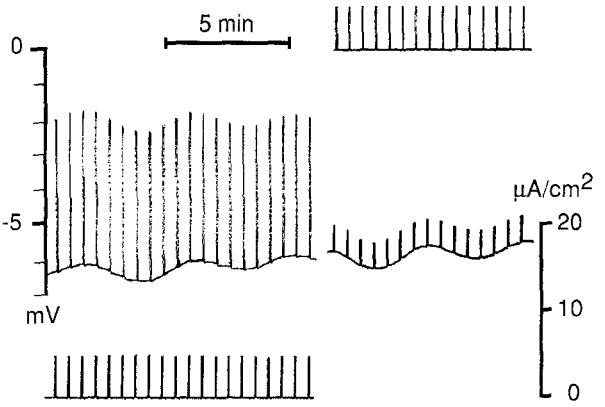

Fig. 2. A typical record from stage 5 HH chick blastoderm at 37°C. *Left:* the transblastodermal potential difference (V_{dorsal}-$V_{ventral}$) obtained when clamping the current to zero (lower trace, pulses 1.2 μA). *Right:* transblastodermal short-circuit current obtained in the same preparation after clamping the transblastodermal potential difference to zero (upper trace, pulses 1.3 mV). The current and voltage pulses were used to determine the total transblastodermal resistance (406 Ω · cm²). The transblastodermal potential, current and resistance show spontaneous and sustained regular oscillations.

μEq/cm²/hr) was again in the dorsoventral direction and equivalent to 3.2 μA/cm². Thus, within the accuracy of the method, the net Na^+ transport accounted for the measured I_{sc} (Table 2*A*).

The values of both $J_{DV}^{Cl^-}$ and $J_{VD}^{Cl^-}$ were about 2 μEq/cm²/hr and not significantly different from each other (Table 2*B*). Ouabain, applied ventrally, did not affect the passage of Cl^- in the dorsoventral direction (Fig. 3).

The Na^+ and Cl^- fluxes across the blastoderm were linearly related (*not shown*) to the total electrical conductance of the preparations. This is illustrated in Fig. 3: after increasing the G_{tot} by means of a gentle mechanical distension of the tissue (a small elevation in the fluid volume of the ventral compartment), the fluxes of both ions increased in parallel.

Ionic Replacements

To identify the ions carrying the I_{sc}, we used selective substitutions of the two principal ions, i.e., sodium and chloride on either side of the embryo.

Replacement of all sodium on both sides of the preparation either by choline or magnesium diminished the values of I_{sc} and V_{oc} to zero and that of G_{tot} by 20% (Table 1 and Fig. 4). Unilateral replacement of all sodium increased or decreased the I_{sc} according to the transblastodermal sodium gradient: when the ventral sodium was replaced, about 30% increase of I_{sc} was observed; when the dorsal sodium was replaced, a negative I_{sc} (i.e., ventrodorsally oriented current) was observed with amplitude corresponding to about 15–30% of the control I_{sc}.

The relationship between the I_{sc} and the sodium concentrations (when identically replaced on both sides, $n = 4$) showed a saturation kinetics with apparent K_m between 25 and 40 mM and I_{max} between 9 and 58 μA/cm² (Fig. 4, inset).

Replacement of all chloride on both sides of the preparation by sulfate, nitrate or gluconate had no significant effect on the I_{sc} but decreased the G_{tot} (Table 1 and Fig. 5). Replacement of all chloride on the dorsal or ventral sides only led to a rapid increase or slow decrease of the I_{sc} showing a higher permeability for chloride in the ventrodorsal direction (Fig. 5).

Measurements in the *Area Opaca* and in the *Area Pellucida*

The parameters described above must reflect the integrated electrical activity of both the *area pellucida* and *area opaca*. Since the structures of both areas are so different from each other (Fig. 1*B* and *C*), we expressed the I_{sc} as a function of the fraction of the studied tissue area occupied by the *area opaca*. The latter parameter was obtained from planimetric measurements in corresponding photographs. As illustrated in Fig. 6, the I_{sc} increased linearly from 14 to 26 μA/cm² when the ratio *area opaca*/total area increased from 20 to 60%.

We have therefore measured in separate experiments the electrical parameters of each area (Fig. 6). The values found in the *area opaca* were: V_{oc} −7.8 ± 1.1 mV, I_{sc} 31.2 ± 12.7 μA/cm², G_{tot} 4.4 ± 2.1 mS/cm²; those found in the *area pellucida* were: V_{oc} − 1.3 ± 0.8 mV, I_{sc} 9.3 ± 4.4 μA/cm², G_{tot} 8.5 ± 4.7 mS/cm².

Removal of Endoderm

Since the *area pellucida* consists of three cell types (Fig. 1*B*), we tried to determine to what extent the endoderm (which is also an epithelial cell sheet) contributes to the observed electrical characteristics. In these measurements, the endoderm and most of the mesodermal cells of one freshly excised blastoderm (stage 5 HH) were carefully dissected out under a binocular microscope. This very fragile preparation was mounted into the chamber in the same manner as described in the previous paragraph using the 2 mm aperture. It consisted mostly of the ectoderm of *area pellucida* and, although more leaky (probably because of mechanical damage), showed V_{oc} of −1.8 mV, I_{sc} of 11.2 μA/cm² and G_{tot} of 6.2 mS/cm², i.e., values within the range found in the whole preparations.

Discussion

Our study shows that the one-day-old chick embryo can be maintained and studied in vitro in short-circuit

Table 2. Fluxes of sodium and chloride

A	J^{Na+}_{DV}	J^{Na+}_{VD} (μEq/cm^2/hr)	J^{Na+}_{net}	I^{Na+}_{net} (μA/cm^2)	I_{sc}
Control	1.07 ± 0.27 *	−0.37 ± 0.05	0.70	18.9	20.3 ± 2.8
n	6	6			12
	*	NS			
Ouabain					
0.1 mM	0.59 ± 0.13 NS	−0.47 ± 0.10	0.12	3.2	1.8 ± 0.4
n	6	4			10
B	$J^{Cl^-}_{DV}$	$J^{Cl^-}_{VD}$ (μEq/cm^2/hr)	$J^{Cl^-}_{net}$		
Control	1.82 ± 0.53	−2.14 ± 0.60	None		
n	4	6			

(A) Dorsoventral (J^{Na+}_{DV}) and ventrodorsal (J^{Na+}_{VD}) fluxes of sodium as calculated from the isotopic flux measurements using 15 min steady-state values for each embryo, in control condition and with ouabain at the ventral side (values are means ± SD). The net fluxes (J^{Na+}_{net}) were calculated by summing the two mean unidirectional fluxes. The net calculated equivalent currents (I^{Na+}_{net}), without and with ouabain, account for the mean I_{sc} actually measured. Notice: 1 μA/cm^2 = 3.7 10^{-2} μEq/cm^2/hr. (*$P < 0.01$; NS: not significant, bilateral unpaired *t*-test).

(B) Dorsoventral ($J^{Cl^-}_{DV}$) and ventrodorsal ($J^{Cl^-}_{VD}$) fluxes of chloride (values are means ± SD). The $J^{Cl^-}_{DV}$ was not significantly different from $J^{Cl^-}_{VD}$.

conditions which, although not physiological, allow to assess the mechanisms of solute and water transfer. In these conditions, the embryo shows epithelial characteristics and performs vectorial transport of positive charges from the dorsal (albumen facing) side to the ventral (yolk facing) side.

Electrical Properties and Ionic Transport across the Chick Blastoderm

Under short-circuit conditions, the blastoderm generates an electrical current of about 20 μA/cm^2 which shows complete dependency on sodium and saturation kinetics. The active component of sodium transport is located at the basolateral membrane of the ectoderm and depends on the ouabain-sensitive Na^+,K^+-ATPase, for at least 80%. The fact that the I_{sc} reached steady-state at all extracellular sodium concentrations used, suggests that the Na^+,K^+-ATPase activity is submaximal and that the factor limiting the sodium transport must be located at the dorsal membrane of the ectoderm. The chloride does not seem to participate in the active transcellular transport as indicated by the fact that replacement of Cl^- by impermeable anions was without effects on the measured I_{sc}.

The transcellular pathway of sodium is responsible for about 20% of the total electrical conductance of the blastoderm (Table 1). A larger part of the conductance is determined by the paracellular pathway through the intracellular junctions. The paracellular conductance is sensitive to mechanical tension (Fig. 3) and allows for passive movements of sodium and chloride across the

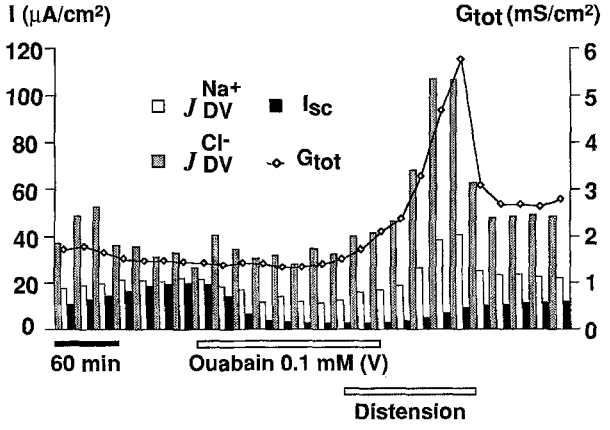

Fig. 3. Transcellular and paracellular flux of sodium. Dorsoventral fluxes of Na^+ ($J^{Na^+}_{DV}$) and Cl^- ($J^{Cl^-}_{DV}$) as determined simultaneously across the same blastoderm (expressed as current equivalent in μA/cm^2) and the response to ventrally (V) applied ouabain. Also represented are the measured I_{sc} and G_{tot}. The first 60 min correspond to the warming of the preparation. The large increase of G_{tot} was induced by a slight distension of the blastoderm.

blastoderm in both directions although not with the same ease, as shown by the results of unilateral replacements of these two ions (Figs. 4 and 5). The large paracellular conductance also explains the relatively modest values of transblastodermal potential difference found under open-circuit conditions (between 3 and 14 mV, ventral side positive).

The ionic transport across the blastoderm seems to be located at the ectodermal cell layer as the removal of endoderm and mesoderm did not modify significantly

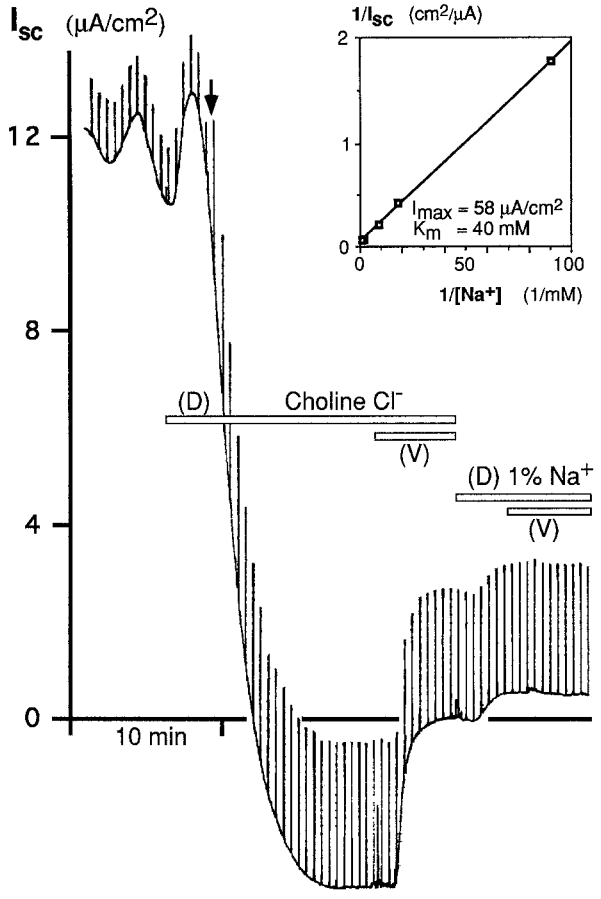

Fig. 4. Effect of sodium replacement by choline. A simultaneous absence of sodium in both the dorsal (*D*) and ventral (*V*) solutions leads to a complete suppression of the short-circuit current (I_{sc}). Arrow: the voltage pulses were increased to facilitate the evaluation of the transblastodermal conductance. When Na^+ (1% of control concentration) was added to the dorsal side, a small increase of I_{sc} was observed. On the ventral side, no significant effect could be detected with this low concentration. *Inset:* example of the kinetics of the sodium transport derived from values obtained by using different symmetrically applied sodium concentrations. The point in the upper right corner corresponds to 1% of the initial sodium concentration.

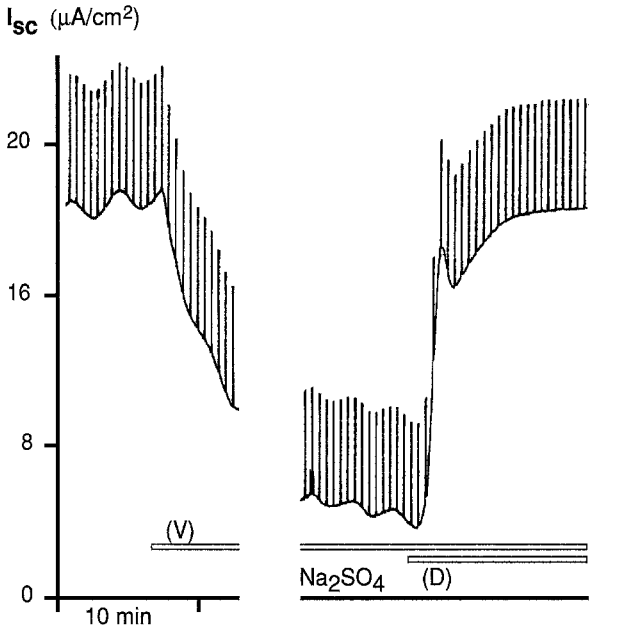

Fig. 5. Effect of chloride replacement by sulfate. A simultaneous absence of chloride in both the ventral (*V*) and dorsal (*D*) solutions does not modify the mean short-circuit current (I_{sc}) but decreases the transblastodermal conductance. Because of a very slow I_{sc} decrease upon dorsal replacement (diffusion of Cl^- in dorsoventral direction), 17 min of the record were cut off.

the electrical properties of the preparation. The endoderm is evidently a very leaky epithelium as it contains many fenestrations (Wakely & England, 1978), and, allows for a rapid penetration of macromolecules, such as IgGs (Kučera & Monnet-Tschudi, 1987).

Comparison with Data Obtained in the Chick

Our data can be compared to some extent with those of Stern and MacKenzie (1983) who penetrated with microelectrodes the stage 3 HH embryos in ovo and measured a transepiblastic potential difference of 16 ± 5 mV which was ventral side positive and ouabain sensitive. Our values which were obtained in vitro, under open-circuit conditions, and in later stages of development (4 HH), confirm such a transcellular polarity and sensitivity to ouabain, but are significantly lower, i.e., −8.9 ± 3.5 mV. This might be due to the use of identical ionic composition on both sides of the preparation (in the egg, the distribution of ions in the fluids bathing the dorsal and ventral ectodermal cell membranes has not been determined but might be asymmetrical (Howard, 1957)). Stern and MacKenzie (1983) also attempted to measure the net Na^+ flux across the chick epiblast. Their value of 4×10^{19} Na^+ atoms/cm²/hr is about 100-fold higher than our result and corresponds to an equivalent current of 1.8 mA/cm². This is a very high current which has not been found in any epithelium.

Comparison with Data Obtained in other Epithelia

The whole chick blastoderm shows a total electrical resistance of 400–500 Ωcm² and can be thus classified in between leaky and tight epithelia according to Frömter and Diamond (1972). Other embryonic preparations show higher values (from 700 Ωcm²; 12–19-day chick allantoic epithelium, Graves, Dunn & Brown, 1,986 to 2,600 Ωcm²; six-day rabbit blastocyst, Cross, 1973).

The transblastodermal potential difference (7.5 mV, ventral side positive) is within the range of values observed in many different embryonic preparation. These potential differences with the same polarity (basal-(in-

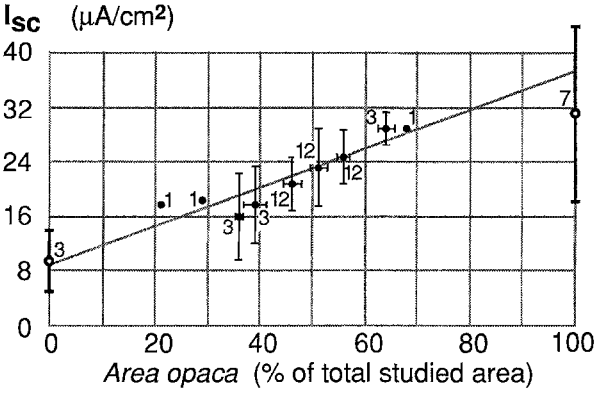

Fig. 6. Dependence of the total short-circuit current on the *area opaca*. The short-circuit current (I_{sc}) increases linearly with the increasing occupancy of the preparation by the *area opaca* (*cf.* Fig. 1*A*). The I_{sc} values found in preparations containing only the *area pellucida* or *area opaca* (open circles) are within the domain predicted by the regression line ($r^2 = 0.85$). The values (means ± SD) are given with the number of determinations.

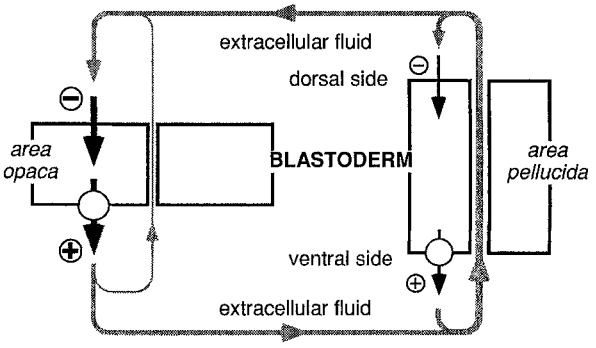

Fig. 7. A model of the electrical properties of the chick blastoderm. The two principal regions of the blastoderm are symbolized by two pairs of ectodermal cells. The tightness of the epithelium is schematized by the narrowness of the intercellular spaces. The transcellular sodium transport (black arrows) consists of a passive entry at the dorsal membrane and active extrusion at the ventral membrane (*cf.* Fig. 5). The transport is more efficient (bold arrows) in the *area opaca* (higher I_{sc}, higher resistance and higher V_{oc}) (*cf.* Fig. 6). Under open-circuit conditions, local differences in electrical properties (positive on the ventral side) are dissipated by pericellular electrical currents (shaded arrows) flowing through the extracellular fluid and the most leaky regions (*area pellucida*).

trablastocoelic)-side positive), vary from 3.84 mV in the 17 day rat visceral yolk sac (Chan & Wong, 1978) to 60 mV in the gastrula of newt (Komazaki & Takada, 1988).

The short-circuit current has been less frequently measured in the mammalian embryos. Values between 5 μA/cm^2 and 19.5 μA/cm^2 were reported (Cross, 1973; Chan & Wong, 1978; Manejwala et al., 1989). This current was always ouabain sensitive but its dependence on sodium seemed to be related to the embryonic age and varied from 5% (six-day rabbit blastocyst, Cross, 1973) to 100% (rat visceral yolk sac, Chan & Wong, 1978; chick allantois 12–19 day, Graves et al., 1986). In the present study, the short-circuit current was fully accounted for by the net sodium transport with a value (about 0.7 μEq/cm^2/hr) which compares with those frequently reported in amphibian epithelia (generally between 0.6 and 2 μEq/cm^2/hr, e.g., Herrera, 1966; Ussing & Zerahn, 1951).

The apparent K_m of the chick transblastodermal sodium transport (between 24 and 40 mM) is within the range of values found in other sodium transporting epithelia of embryonic type (e.g., 20 mM in the visceral yolk sac of the rat, Chan & Wong, 1978; about 37 mM in the preimplantation mouse embryo, Manejwala et al., 1989) or mature type (e.g., 6–25 mM in the skin of various frogs, cited in Ehrenfeld and Garcia-Romeu, 1980).

Electrical Heterogeneity within the Blastoderm

Clearly, the *area opaca* is tighter and responsible for a higher short-circuit current than the *area pellucida* (Fig. 6). In open-circuit conditions, both areas are electrically connected by conductive extracellular fluid and must be therefore at the same potential (principle of electroneutrality). This means that any potential difference built up locally in both areas is dissipated by extracellular electrical currents (Fig. 7). This is indeed the case: such currents were mapped over the whole blastoderm using a computer-controlled vibrating probe (Kučera & de Ribaupierre, 1989). In blastoderms surrounded by the vitelline membrane, the pericellular electrical currents showed a characteristic radial pattern: the current loops diverged from the ventral face of the *area opaca* and returned around the margin of the blastoderm (i.e., through the very leaky vitelline membrane) to the dorsal face. A weaker current loop converged through a relatively leaky region situated in front of the primitive streak (Kučera & de Ribaupierre, 1989).

This aspect deserves special attention. In homogeneous epithelia studied in Ussing type chambers, it is widely accepted that, under open-circuit conditions, a net transport of charges is small and compensates for the back-leak through the paracellular conductance because there is no other possibility of leak between the two compartments of the chamber. In such conditions, a steady-state is achieved across the epithelium similar to a situation determining the resting potential across a cell membrane. However, when the apical and basal compartments are connected through low resistance regions such as the *area pellucida* or vitelline membrane, like in the blastoderm in ovo, the charges accumulated by the transcellular transport on the basal side are continuously dissipated by spatially organized pericellular currents. Such currents have been also found in matured but functionally inhomogeneous epithelium of intestinal villi (Holtug et al., 1991).

In conclusion, the experiments presented in this paper show that the developing chick embryo can be readily and reproducibly studied in a perfusion chamber under short-circuit conditions. The early chick blastoderm is an epithelium-like organism and contains regions with different transporting properties. Under open-circuit conditions, it represents from a thermodynamical point of view a complex supracellular dissipative structure. Moreover, it is continuously differentiating which allows to follow the expression and maturation of individual transport pathways. This aspect, namely, the identification of transporters involved in the ionic movements across the blastoderm, is discussed in a second paper (Abriel, Katz & Kučera, 1994).

This work was supported by the Swiss National Research Foundation (grant. 3.418-0.86 to P.K.) and by Roche Research Foundation (grant. to U.K.). We thank Drs. E. Raddatz and Y. de Ribaupierre for helpful discussions.

References

Abriel, H., Katz, U., Kučera, P. 1994. Ion transport across the early chick embryo: II. Characterization and pH sensitivity of the transembryonic short-circuit current *J. Membrane Biol.* **141:** 159–166

Balinsky, B.I. 1981. An Introduction to Embryology. Fifth edition. pp. 208–246 and 333–343. Holt-Saunders, Japan

Benos, D.J. 1981. Developmental changes in epithelial transport characteristics of preimplantation rabbit blastocysts. *J. Physiol.* **316:** 191–202

Borland, R.M. 1977. Transport processes in the mammalian blastocyst. *Dev. Mammals* **1**:31–67

Chan, S.T.H., Wong, P.Y.D. 1978. Evidence of active sodium transport in the visceral yolk sac of the rat in vitro. *Physiology* **279:** 385–394

Cross, M.H., Brinster, R.L. 1970. Influence of ions, inhibitors and anoxia on transtrophoblast potential of rabbit blastocyst. *Exp. Cell Res.* **62:**303–309

Cross, M.H. 1973. Active sodium and chloride transport across the rabbit blastocoele wall. *Biol. Reprod.* **8:**566–575

DiZio, S.M., Tasca, R.J. 1977. Sodium-dependent amino acid transport in preimplantation mouse embryos. III. Na^+-K^+-ATPase linked mechanism in blastocysts. *Dev. Biol.* **59:**198–205

Ehrenfeld, J., Garcia-Romeu, F. 1980. Kinetics of ionic transport across the frog skin: Two concentration-dependent processes. *J. Membrane Biol.* **56:**134–147

Fleming, T.P., McConnell, J., Johnson, M.H., Stevenson, B.R. 1989. Development of tight junctions de novo in the mouse early embryo: Control of assembly of the tight junction-specific protein, ZO-1. *J. Cell Biol.* **108:**1407–1418

Frömter, E., Diamond, J. 1972. Route of passive ion permeation in epithelia. *Nature New Biol.* **235:**9–13

Graves, J. S., Dunn, B. E., Brown, S. C. 1986. Embryonic chick allantois: functional isolation and development of sodium transport. *Am. J. Physiol.* **251:**C787–C794

Hamburger, V., Hamilton, H. 1951. A series of normal stages in the development of the chick embryo. *J. Morphol.* **88:**49–92

Herrera, F.C. 1966. Action of ouabain on sodium transport in the toad urinary bladder. *Am. J. Physiol.* **210:**980–986

Holtug, K., Shipley, A., Dantzers, V., Sten-Knudsen, O., Skadhauge, E. 1991. Localization of sodium absorption and chloride secretion in an intestinal epithelium. *J. Membrane Biol.* **122:**215–229

Howard, E. 1957. Ontogenetic changes in the freezing point and sodium and potassium content of the subgerminal fluid and blood plasma of the chick embryo. *J. Comp. Physiol.* **50:**451–470

Komazaki, S., Takada, M. 1988. Amiloride-sensitive potential difference across the blastocoelic wall of early embryos of the newt, *Cynops pyrrhogaster*. *Comp. Biochem. Physiol.* **91A:**129–133

Kučera, P., Burnand, M.-B. 1987. Mechanical tension and movement in the chick blastoderm as studied by real-time image analysis. *J. Exp. Zool.* **S1:**329–339

Kučera, P., de Ribaupierre, Y. 1989. Extracellular electrical currents in the chick blastoderm. *Biol. Bull.* **176(S):**118–122

Kučera, P., Katz, U. 1988. Sodium current clock in the early chick embryo. *Experientia* **44:***A*34 (*Abstr.*)

Kučera, P., Monnet-Tschudi, F. 1987. Early functional differentiation in the chick embryonic disc: interaction between mechanical activity and extracellular matrix. *J. Cell Sci.* **S8:**418–431

Kučera, P., Raddatz, E. 1980. Spatio-temporal measurements of the oxygen uptake in the developing chick embryo. *Resp. Physiol.* **39:** 199–215

Kučera, P., Raddatz, E., Baroffio, A. 1984. Oxygen and glucose uptakes in the early chick embryo. *In:* Respiration and Metabolism of Embryonic Vertebrates. W. Seymour, editor. pp. 299–309. Junk Publ., Dordrecht, Boston, London

Manejwala, F.M., Cragoe, E.J., Schultz, R.M. 1989. Blastocoel expansion in the preimplantation mouse embryo: role of extracellular sodium and chloride and possible apical routes of their entry. *Dev. Biol.* **133:**210–220

Morill, G.A., Kostellow, A.B., Watson, D.E. 1966. The electropotential difference between the blastocoel and the external medium in the amphibian embryo: Its similarity to adult frog trans-skin potential. *Life Sci.* **5:**705–709

Powers, R.D., Borland, R.W., Biggers, J.D. 1977. Amiloride-sensitive rheogenic Na^+ transport in rabbit blastocyst. *Nature* **270:**603–604

Raddatz, E., de Ribaupierre, Y., Kučera, P. 1987. Micromeasurements of total and regional CO_2 productions in the one-day old chick embryo. *Resp. Physiol.* **70:**1–11

Raddatz, E., Kučera, P. 1983. Mapping of the oxygen consumption in the gastrulating chick embryo. *Resp. Physiol.* **51:**153–166

Romanoff, A.L. 1967. Biochemistry of the Avian Egg. pp. 202–229. Wiley, New York

Simkiss, K. 1980. Water and ionic fluxes inside the egg. *Amer. Zool.* **20:**385–393

Smith, M.W. 1970. Active transport in the rabbit blastocyst. *Experientia* **26:**736–738

Stern, C.D., MacKenzie, D.O. 1983. Sodium transport and the control of epiblast polarity in the early chick embryo. *J. Embryol. Exp. Morphol.* **77:**73–98

Stern, C.D., Manning, S., Gillespie, J.I. 1985. Fluid transport across the epiblast of the chick embryo. *J. Embryol. Exp. Morphol.* **88:** 365–384

Ussing, H.H., Zerahn, K. 1951. Active transport of sodium as the source of electric current in the short-circuited isolated frog skin. *Acta Physiol. Scand.* **23:**110–127

Wakely, J., England, M.A. 1978. Development of the chick embryo endoderm studied by S.E.M. *Anat. Embryol.* **153:**167–178

Wiley, L.M. 1984. Cavitation in the mouse preimplantation embryo: Na/K-ATPase and the origin of nascent blastocoele fluid. *Dev. Biol.* **105:**330–342